Bearing fault diagnosis for electric machines using motor current signals and state classification

Dang Huu Hai[1], Bui Ngoc My[2], Hoang Van Phuc[3], Bui Quy Thang[3*], Le Thi Huyen[4]

[1]Institute of Electronics, Academy of Military Science and Technology;
[2]Department of Training, Academy of Military Science and Technology;
[3]Institute of System Integration, Le Quy Don Technical University;
[4]Naval Technical Institute.
[*]Corresponding author: bqthangcndt@gmail.com

Received 28 Mar. 2023; Revised 25 Jun. 2023; Accepted 08 Aug. 2023; Published 25 Aug. 2023.
DOI: https://doi.org/10.54939/1859-1043.j.mst.89.2023.15-24

ABSTRACT

Procedures for diagnosing bearing failures of induction motors based on motor current signals in published methods commonly denoise signals acquired from current sensors, then extract the typical characteristics from the denoised signals, and use a classifier to discriminate the state of bearing. However, the current signals in practice could be affected by surrounding noises, creating extraordinary peaks in the signals which may lead to an inaccurate diagnostic result. Thus, the traditional methods may not be very effective in diagnosing failures for induction motors using motor current signals in real-time. To mitigate these issues, this work introduces a new technique, which consists of characterizing the bearing health as a state vector composed of signal features, evaluating the real bearing status from the characteristic-space using a Kalman filter and a k-NN classifier. This technique still achieves quite high precision even in noisy condition. Experimental results with noise-adding signals demonstrate that the proposed technique has a mean proper identification proportion of 92.06% and a mean false proportion of 7.94%, while the conventional ones turn out a maximum mean true identification proportion of 53.12% and a minimum mean mistake proportion of 46.88%.

Keywords: Bearing fault diagnosis, motor current signal, state classification.

1. INTRODUCTION

Rotating electric machines in general and electric motors in particular play a very significant role in industries. Motor failures are commonly categorized into four subjects: bearing, stator, rotor and other failures, in which bearing faults account for the largest percentage in total, greater 40% according to research by General Electric Co and IEEE-IGA [1]. Hence, bearing fault diagnosis is important for the health monitoring of rotation machinery.

Until now, numerous techniques have already researched and published to monitor and classify bearing defects, which are vibration analysis, electromagnetic field supervision, motor current signal analysis (MCSA), analysis of the acoustic signal analysis. Bearing fault diagnosis based on vibration signal has been published by many scientists; however, the vibration method requires to install costly vibration sensors. Moreover, the challenging arrangement of such sensors at the efficient locations as well as the difficulties in construction space to acquire the best vibration signals, which expose bearing condition the most accurately, is another disadvantage of the vibration method. Additionally, apart from collecting signals from the testing motor, vibration sensors may acquire signals coming from other nearby machines, which are considerable noise sources. In contrast to the above imperfection of the vibration method, the MCSA owns several advantages to attract the interest of researchers and scientists in fault diagnosis for bearings. First, no additional sensor is required because MCSA uses the current signal after inverter block of the engine; as a result, its cost is reduced as well as its system design is less complex than the vibration method. Furthermore, the MCSA method can be applied to observe a huge number of engines from only one place utilizing motor current (MC) signals while it is challenging if using the vibration method due to the interference with surrounding noise.

Commonly, diagnosis of bearing failures based on current or vibration data consists of two stages: feature extraction and fault classification. Several techniques used in the characteristic extraction are Fast Fourier Transform (FFT) [2], Discrete Wavelet Transform (DWT) [2], Empirical Mode Decomposition (EMD) [3], Local Mean Decomposition (LMD) [4], and Variational Mode Decomposition (VMD) [5]. Some typical classification techniques comprise support vector machine (SVM) [6], convolutional neural network (CNN) [7], K-Nearest Neighbor (*k*-NN) [8].

The above techniques all consist of steps: denoising signals, extracting and selecting appropriate characteristics, and finally classifying conditions with a classifier trained by selected characteristics. This way can bring about high accuracy; however, for real-time applications, the published methods may be unsuitable due to their computational complexity. In addition, if fault symptoms are deeply buried by noise, traditional methods may no longer be effective. Thus, this paper proposes a new technique to overcome the current disadvantages of the previous methods for detecting bearing failures in an induction motor. In this study, we denoise and extract the features from current signal. Later, the system condition is estimated using a Kalman Filter. After that, some optimal features are selected for training the *k*-NN classifier. Finally, an effectiveness comparison of the proposed method to the traditional techniques is made. Therefore, the main contributions of this paper are as follows:

1. Proposing a method to improve fault diagnosis efficiency using a Kalman Filter to estimate system status in characteristic-space instead of signal-space.
2. Using a *k*-NN classifier to contrast the effectiveness of the suggested technique to the published methods.
3. Verifying the effectiveness of the proposed method through various experiments with both noise-added and no-noise signals.

2. DAMAGE DIAGNOSIS TECHNIQUE

Figure 1 demonstrates the method presented in this article which contains offline analysis and real-time implementation to diagnose bearing failures. The offline analysis stage defines the feature set of the MC signal that will be used for fault diagnosis and detection. Once defined, these features can then be extracted from MC signals acquired by another IM in reality and utilized to diagnose the failure of any bearing in that IM - this is a second stage of the proposed technique, that mean real-time execution stage. In general, offline analysis involves steps such as recording MC signals, segmenting them into signal frames, extracting features from each of those frames, and selecting optimal features to determine the feature set for fault diagnosis.

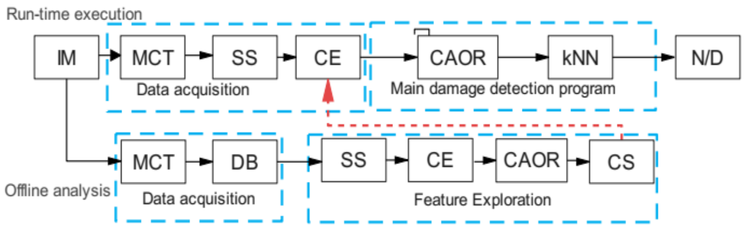

***Figure 1**. Overall diagram of detecting damage in bearings using MC signals (IM: Induction motor, MCT: The transducer to collect MC, SS: Signal split, CE: Characteristic extraction, CAOR: Condition assessment and outlier removal, CS: Characteristic selection, DB: Data base, N/D: Normality/damage, k-NN: k nearest neighbors).*

MC signals are acquired using a current transducer installed after the frequency inverter on the motor system needs to diagnose fault in bearings. Signal segmentation is detailly discussed in subsection 2.1. Extracting the features will be implemented in each frame, the main fault diagnostic program then uses the Kalman filter to assess the real status in bearings in the characteristic-space. In fact, the MC signal samples acquired from the current transducer always include measurement noise and interference from external sources, creating anomalies in the signals. The role of state estimation block is to eliminate these anomalies, predict the next state of the system close to the real state of the system, thereby increasing the accuracy of state classification. In order to reduce the complexity of calculations and save resources, our method only selects the optimal and specific features. Less specific features to bearing states are omitted. Classification step uses the *k*-NN classifier to classify the bearing condition as failure or normal.

2.1. Signal segmentation

The MC signals obtained from a running motor are non-stationary. They are affected by a variety of causes such as bearing failures, installation defects that cause the magnetic gap to shift, or effects from other components which share the same source system with the engine. Therefore, the MC signals should be analyzed over various durations by separating the signals into sequential overlapping frames and then extracting characteristics from those frames. This helps to minimize the impact of instability on extracted characteristics. Fig. 2 depicts the long MC signal and a frame of it. The length of a frame is a perfect square depends on sampling frequency, rotary speed value.

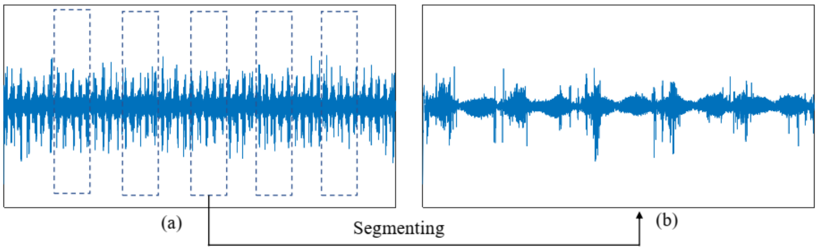

***Figure 2**. Signal split: (a) The signal from MCT, (b) A segment of long signal.*

2.2. Feature Extraction

There are many time and frequency domain statistical features are used to detect the condition of bearing. Table 1 lists sixteen the most typical features are extracted from each frame of MC signal to create a feature group for the next signal processing step. Extracted features are put into the state estimation and noise rejection module. State estimation and noise removal are detail discussed in Section 2.3.

***Table 1.** Characteristic features for fault diagnostic [9].*

Feature	Equation	Feature	Equation
Short time energy (STE)	$\sum_{m=1}^{M} x_m^2$	Shape factor (SHF)	$\mathrm{RMS}/\frac{1}{M}\sum_{m=1}^{M}\lvert x_m\rvert$
Root mean square (RMS)	$\sqrt{(\sum_{m=1}^{M} x_m^2)/M}$	Crest factor (CRF)	$\max(\lvert x\rvert)/RMS$
Average amplitude (AVA)	$\frac{1}{M}\sum_{m=1}^{M}\lvert x_m\rvert$	Square-mean-root (SMR)	$\left(\frac{1}{M}\sum_{m=1}^{M}\sqrt{\lvert x_m\rvert}\right)^2$
Spectral peak (SPP)	$\underset{f}{\mathrm{argmax}}(X(f))$	Clearance factor (CLF)	x_{peak}/SMR
Spectral spread (SPS)	$\sqrt{(\sum_{m=1}^{M}(f_m - f_c)^2 X_m^2/(\sum_{m=1}^{M} X_m^2)}$	Impulse factor (IMF)	$\max(\lvert x\rvert)/\frac{1}{M}\sum_{m=1}^{M}\lvert x_n\rvert$

Feature	Equation	Feature	Equation
Kurtosis (KUR)	$\sum_{m=1}^{M}\left((x_m-\mu)/\sigma\right)^4/M$	Shape factor square-mean-root (SFSMR)	$SMR/\frac{1}{M}\sum_{m=1}^{M}\lvert x_m\rvert$
Entropy (ETY)	$-\sum_{m=1}^{M}q_m\log_2 q_m$	5th normalized moment (NM5)	$\frac{1}{M}\sum_{m=1}^{M}\left(\frac{x_m-\bar{x}}{\sigma}\right)^5$
Spectral centroid (SPC, fc)	$\sum_{m=1}^{M}f_m X_m^2/\sum_{m=1}^{M}X_m^2$	6th normalized moment (NM6)	$\frac{1}{M}\sum_{m=1}^{M}\left(\frac{x_n-\bar{x}}{\sigma}\right)^6$
where, x_m*'s* ($m=1,....,M$) are M samples of a frame of the input data; f is the frequency; X is the short period of time spectrum amplitude; μ and σ are average and standard deviation of x; $\sigma=\sqrt{\frac{1}{M}\sum_{m=1}^{M}(x_m-\bar{x})^2}$, $q_m=x_m^2/\sum_{m=1}^{M}x_m^2$			

2.3. Condition Assessment and Outlier Removal

We define the state space equation of the system in characteristic space as follows:

$$\mathrm{x}_{n+1}=\mathrm{F}_n\mathrm{x}_n+\mathrm{w}_n,\quad \mathrm{z}_n=\mathrm{C}_n\mathrm{x}_n+\mathrm{v}_n \tag{1}$$

Where, F_n is status transformation matrix, its size is ($n_x \times n_x$); C_n is measuring matrix, its size is ($n_z \times n_x$); n is the discrete-time index; $\mathbf{x}_n$ shows the status vector of bearings, the size of this vector is ($n_x \times 1$); $\mathbf{z}_n$ indicates the supervision vector it is formed by selected features, the size of this vector is ($n_z \times 1$); $\mathbf{w}_n$ is process interference vector, its size is ($n_x \times 1$); $\mathbf{v}_n$ is measuring interference vector, its size is ($n_z \times 1$). In our work, $\mathbf{x}_n$ is a vector containing elements of 0, 1 or 2 if the bearing has no fault, outer race faults or inner race faults, respectively.

The covariance matrices for the $\mathbf{w}_n$ and $\mathbf{v}_n$ vectors are given by:

$$E\left[\mathrm{w}_n\mathrm{w}_i^T\right]=\begin{cases}\mathrm{Q}_n, i=n\\ 0, i\neq n\end{cases}, E\left[\mathrm{v}_n\mathrm{v}_i^T\right]=\begin{cases}\mathrm{R}_n, i=n\\ 0, i\neq n\end{cases}, E\left[\mathrm{w}_n\mathrm{v}_i^T\right]=0\,\forall\; n,i \tag{2}$$

Where, T denotes the matrix transpose, E[.] denotes expectation function, $\mathbf{Q}_n$ is the process noise covariance, $\mathbf{R}_n$ is the measurement noise covariance. Measuring interference $\mathbf{v}_n$ can include intrinsic interference sources such as defects in the manufacture and installation of bearings, roller, drive shaft. Reality, the noise sources do not express the failure in bearings. Consequently, $\mathbf{v}_n$ in (1) mainly describes the internal noise sources and they exist only during the rotating machine operation. In accord with (1), if the bearing is in normal operation $\mathbf{x}_n$ is a vector containing elements of 0, and $\mathbf{z}_n$ turns into $\mathbf{v}_n$. Therefore, we could examine the normal-state measurement noise $\mathbf{v}_n$ and implement it to monitor bearing status of rotating machines assuming this noise source is steadfast before and after bearing failure.

Next, we apply a linear Kalman filter [10, 11] for the system model in (1) for status assessment. The condition estimate graph is shown in Fig. 3. Kalman gain K is calculated as the first step in processing an estimate utilizing the $\mathbf{R}_n$ and the related error covariance P_n^- provided by:

$$\mathrm{P}_n^-=E\left[\mathrm{e}_n^-\mathrm{e}_n^{-T}\right];\mathrm{e}_n^-=\mathrm{x}_n-\hat{\mathrm{x}}_n^- \tag{3}$$

Where, $\hat{\mathrm{x}}_n^-$ shows the predicted state, e_n^- shows the prediction error. Next, the status assessment $\hat{\mathrm{x}}_n$ is updated by using the Kalman gain $\mathbf{K}$ and the observation $\mathbf{z}_n$*;* then we can calculate the error covariance $\mathbf{P}_n$ defined as follows:

$$\mathrm{P}_n=E\left[\mathrm{e}_n\mathrm{e}_n^T\right];\mathrm{e}_n=\mathrm{x}_n-\hat{\mathrm{x}}_n \tag{4}$$

Where, $\mathbf{e}_n$ is the error of the assessment.

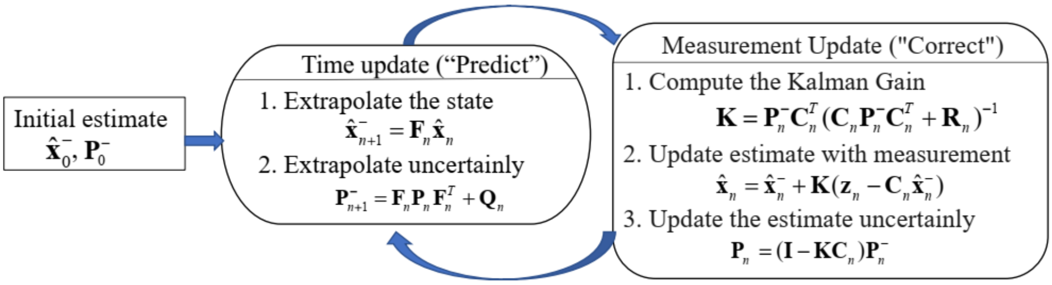

***Figure 3.** Graph of status assessment (**I** is the unit matrix).*

A next condition is predicted with the assessed value $\hat{x}_n$, $\mathbf{P}_n$, and $\mathbf{Q}_n$, and the assessment process reiterates. Initializing the values $\hat{x}_0^-, P_0^-$ is fundamental step of the status assessment process. As mentioned above, we could inspect the measurement interference in the normal condition of the bearings. As a result, $\hat{x}_0^-$ and P_0^- could be defined by:

$$\hat{x}_0^- \approx \hat{z} = \frac{1}{N}\sum_{j=-N}^{-1} z_j;\ P_0^- = E[e_o^- e_o^{-T}] = R_0 \approx \frac{1}{N}\sum_{j=-N}^{-1}(z_j - \bar{z})((z_j - \bar{z})^T \quad (5)$$

Where $\mathbf{z}_j$'s, j = -N, -N+1,….,-1 are N previous measurements and $e_0^- = x_0 - \hat{x}_0^-$ is the initial assessment error and $\mathbf{R}_0$ is its covariance matrix.

2.4. Feature Selection

To reduce computational complexity and improve damage detection precision of the suggested technique, we only choose some important features that are obtained from estimating the condition to diagnose bearings fault. The criteria to rank the importance of each feature founded on the Fisher's discriminant ratio (FDR) [12] defined by:

$$\mathrm{FDR} = \frac{(\mu_0 - \mu_1)^2}{\sigma_0^2 + \sigma_1^2} \quad (6)$$

Where, μ_0, σ_0^2 and μ_1, σ_1^2 are the average and variance of the characteristic of normality status and abnormal status in bearings, respectively. The larger FDR, that feature is more important.

2.5. State classification

With those selected features from previous step, a k-NN classifier is used to distinguish the normality status from the outer race fault state or the inner race fault state, in which we use the Euclidean function [13] to calculate distance between two data points:

$$\alpha_j = \sqrt{\sum_{n=1}^{k}(w_n - x_{n,j})^2} \quad (7)$$

Where α_j is Euclidean distance between the input characteristic vector w = {$w_1, w_2, \ldots, w_k$} and the j^{th} training vector $x_{*j} = \{x_{1j}, x_{2j}, \ldots, x_{kj}\}$, $j = 1, 2, \ldots, N$. The classifier based on *k-NN* algorithm sorts the input w into the main label in its k nearest neighbors corresponding to k minimum distances α_j $(k < N)$.

3. RESULTS AND DISCUTION

3.1. Input data

We utilize the bearing dataset provided by a test rig which is invented at the Chair of Design and Drive Technology, Paderborn University [14] to demontrate our proposed technique. Fig. 4 depicts the setup of the testing bench. There are five main parts in the testing bench: a motor powered by electricity, a torque-measurement rod, a module to test bearing, a flywheel, and a load motor. There is a dataset of 32 bearing codes consists of 6 no faul bearing codes (K001-K006), 12 outer race fault bearing codes (KA01, KA03-KA09, KA15, KA16, KA22, KA30), 11 inner race fault bearing codes (KI01, KI03-KI05, KI07, KI08, KI14, KI16-KI18, KI21) and 3 inner race and outer race fault bearing codes (KB23, KB24, KB27). The motor has 4 working conditions. There are 20 measurements were implemented with each bearing code of each working condition of the motor. There is a matlab file contains the data of each measurement includes the radial force (F), the torque (M), the speed (S), the vibration signal, the oil temperature of bearing module, the phase 1 current signal (PH1), and the phase 2 current signal (PH2). In this article, we utilize the PH1 of fifteen bearing codes in table 2 in which the working condition of electric motor is considered as rotational speed of the electric motor (S) = 900 rpm, the load torque of the load motor (M) = 0.7 Nm and the radial force on the test bearings (F) = 1000 N to demonstrate our proposed method.

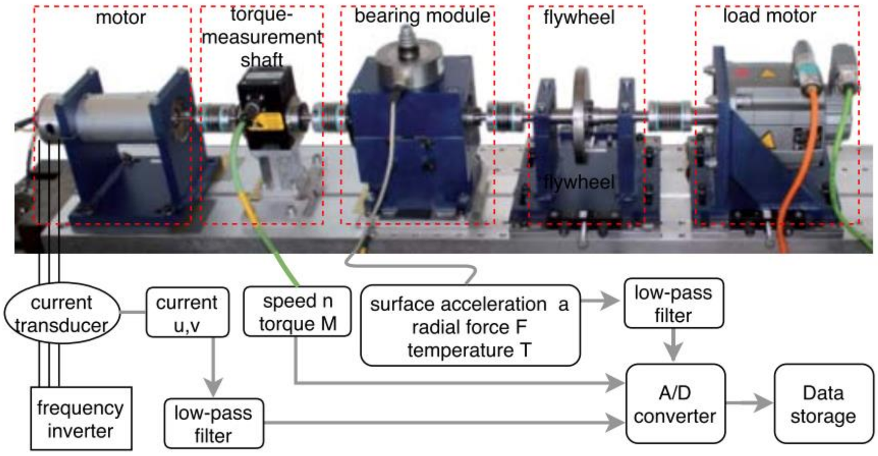

Figure 4. *Schematic of signal measurement [14].*

Table 2. *Bearing codes are utilized for taking data [15].*

Condition of bearings	Class	Label	Used bearing code
No fault (N)	0	K0	K001, K002, K003, K004, K005
Outer race fault (O)	1	KA	KA04, KA15, KA16, KA22, KA30
Inner race fault (I)	2	KI	KI04, KI14, KI16, KI18, KI21

3.2. Methods, simulation tools

In the offline phase, first of all, the data set of current signals of the same motor corresponding to five bearing codes of each the bearing label in table 2 are divided into segments. The signal length of a measuring of five bearing codes for label 0, label 1 and label 2 is 1284915, 1280176 and 1280002, respectively. The size of the signal frame (L) is 6400 [15]. Therefore, the number of frames for each label of a measuring is rounded as 200. Feature extraction is implemented in each frame of each bearing label using sixteen equations in table 1 with the raw signal, the DWT technique, the EMD technique and the our recommended method. There are 20 measurings for each bearing code. Therefore, the lengh of each feature for each label of bearings in table 2 is 4000 samples. After estimating the condition, we select ten important features has the highest FDR scores to diagnose bearings fault. Finally, we use the *k*-NN classifier is trained by ten optimal characteristics to evaluate the efficiency of the our suggested technique contrast to the existing methods consist of DWT and EMD. With the number of samples is not too big, we utilized 80% of 4000 samples of each label for training and the remaining 20% for testing to ensure the precision of the trained model. We implement this procedue with both the noise-adding signal and no-noise signal to show the efficiency of the our proposed method. The whole process of calculation and simulation is done using Matlab tool on a personal computer with an Intel (R) core i5 2.5 GHz processor, and 8 GB RAM.

3.3. Simulation results and comments

Table 3 and table 4 show the FDR scores when applying (6) for 16 features in table 1 are extracted from signals denoised by EMD method, DWT method and the proposed method with no-noise signals and noise-adding signals respectively of the same data set for K0, KA and KI bearing labels in table 2.

Table 3. *FDR scores of the features are extracted by different methods with no-noise signal.*

Feature	K0-KA				K0-KI			
	Raw Signal	**EMD Method**	**DWT Method**	**Proposed Method**	**Raw Signal**	**EMD Method**	**DWT Method**	**Proposed Method**
STE	0.0216	0.0298	0.0232	0.2035	0.0487	0.0527	0.0189	0.8349
RMS	0.0282	0.0427	0.0365	0.2585	0.0550	0.0683	0.0345	0.8648
AVA	0.0158	0.0306	0.0378	0.1039	0.0585	0.0755	0.0419	0.7472
SPP	0.0005	0.0002	0.1056	0.0265	0.0000	0.0000	0.1144	0.2781
SPS	0.0032	0.0000	0.0157	4.3875	0.0423	0.0001	0.0170	4.3193
KUR	0.0258	0.0107	0.0121	0.5035	0.0709	0.0004	0.0295	1.5641
ETY	0.0007	0.0000	0.0103	0.8458	0.0005	0.0012	0.0010	1.0524
SPC	0.0020	0.0034	0.0919	0.0017	0.0295	0.0255	0.0691	0.5979
SHF	0.0351	0.0018	0.0319	0.5902	0.0321	0.0009	0.0430	0.9551
CRF	0.0282	0.0004	0.1075	5.0883	0.0341	0.0024	0.1072	3.7651
SMR	0.0040	0.0185	0.0198	0.0125	0.0447	0.0574	0.0352	0.5810
CLF	0.0054	0.0000	0.0354	1.8724	0.0086	0.0002	0.0517	0.9080
IMF	0.0084	0.0000	0.0875	2.6596	0.0120	0.0005	0.0881	1.4267
SFSMR	0.1172	0.0128	0.0371	1.7157	0.0893	0.0107	0.0141	1.9080
NM5	0.0014	0.0000	0.0018	2.3318	0.0022	0.0000	0.0020	1.8086
NM6	0.0000	0.0001	0.0737	0.5951	0.0005	0.0003	0.0765	0.0898

Table 4. *FDR scores of the features are extracted by different methods with noise-adding signal.*

Feature	K0-KA				K0-KI			
	Raw Signal	**EMD Method**	**DWT Method**	**Proposed Method**	**Raw Signal**	**EMD Method**	**DWT Method**	**Proposed Method**
STE	0.0008	0.0044	0.0007	0.0000	0.2420	0.2953	0.0000	2.4302
RMS	0.0008	0.0046	0.0025	0.0000	0.2479	0.2970	0.0017	2.4218
AVA	0.0003	0.0027	0.0020	0.0030	0.3475	0.3244	0.0024	2.3421
SPP	0.0009	0.0002	0.0006	0.1383	0.0000	0.0000	0.0001	0.2705
SPS	0.0103	0.0000	0.0012	2.2669	0.0148	0.0000	0.0008	2.3267
KUR	0.0016	0.0038	0.0004	0.0187	0.1662	0.1128	0.0010	2.4710
ETY	0.0003	0.0040	0.0007	0.0031	0.0005	0.0000	0.0011	0.3029
SPC	0.0055	0.0004	0.0002	0.5896	0.0007	0.0014	0.0000	0.4161
SHF	0.0078	0.0066	0.0009	0.2079	0.0051	0.0034	0.0004	0.4010
CRF	0.0000	0.0015	0.0000	0.1364	0.0009	0.0000	0.0001	0.0491
SMR	0.0005	0.0018	0.0000	0.0061	0.3532	0.3167	0.0013	2.2541
CLF	0.0000	0.0016	0.0005	0.0921	0.0006	0.0000	0.0001	0.0218

Feature	K0-KA				K0-KI			
	Raw Signal	EMD Method	DWT Method	Proposed Method	Raw Signal	EMD Method	DWT Method	Proposed Method
IMF	0.0000	0.0015	0.0000	0.1030	0.0006	0.0000	0.0000	0.0287
SFSMR	0.0072	0.0046	0.0077	0.2060	0.0037	0.0026	0.0036	0.5629
NM5	0.0003	0.0000	0.0011	1.7356	0.0005	0.0000	0.0009	1.6770
NM6	0.0004	0.0000	0.0008	0.0718	0.0000	0.0000	0.0016	0.1927

Based on table 3, it could be shown that although the input signal samples do not have noise, the existing signal denoising techniques do not improve the label separability, and even reduce some characteristics according to their FDR scores. For instance, SPS, ETY, CLF, IMF, NM5 features of denoised signals using EMD method have smaller FDR scores than the scores of those features for Raw signal when comparing K0 code to KA code. By contrast, the proposed technique has remarkably larger FDR scores for all the features as presented in table 1. Similarly, table 4 demonstrates that with the noise-adding signals, almost features of denoised signals using DWT method have smaller FDR scores than the scores of those features for Raw signal when comparing K0 code to KI code whereas suggested method has still bigger FDR scores for all the features.

To evaluate failure classification accuracy between K0 and KA, and between K0 and KI for different signal preprocessing methods of the same data set, we apply *k-NN* classification model trained by two optimal feature groups of normal bearing status and abnormal bearing status. Fig. 5 and Fig. 6 depict confusion matrix of different signal preprocessing methods for *k*-NN classifier with both the no-noise signal and noise-adding signal, correspondingly.

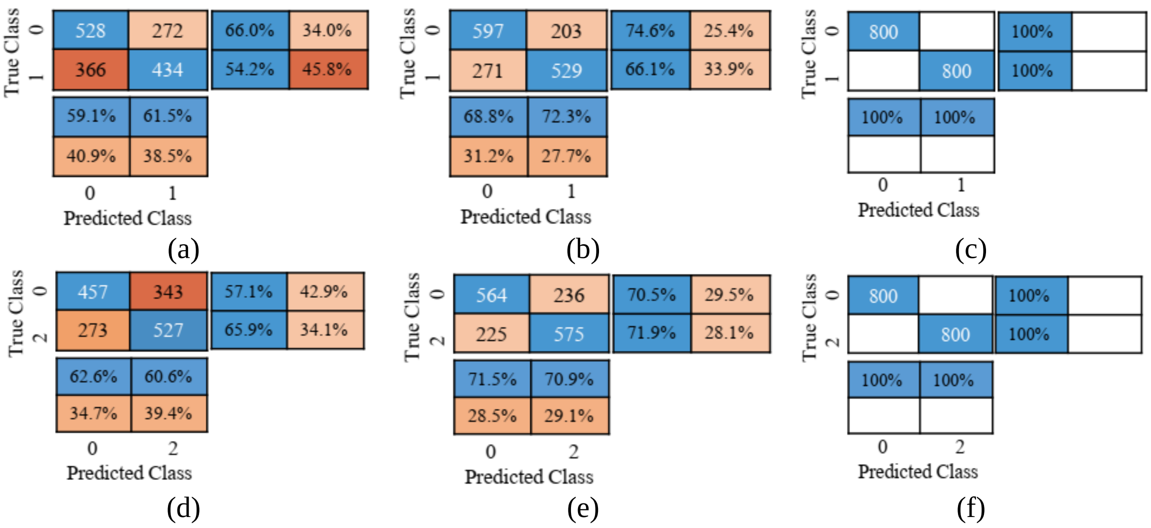

Figure 5. *Confusion matrix of k-NN classifier by different methods: (a) K0-KA, DWT, (b) K0-KA, EMD, (c) K0-KA, the proposed method, (d) K0-KI, DWT, (e) K0-KI, EMD, (f) K0-KI, the proposed method with the no-noise signal.*

Next, we compare the fault diagnosis correctness of the published signal denoise techniques to the proposed method. The correctness (ACC) is computed by:

$$ACC = (TZ+TF)/(Z+F)*100\% \quad (8)$$

Where, Z is the quantity of the no fault bearing signal specimens which are used to test; F is the quantity of inner or outer race fault bearing signal specimens which are used to test; TZ is the quantity of bearing signal specimens for which the classifier gives no fault; TF is the quantity of bearing signal specimens for which the classifier gives the inner race fault or the outer race fault.

Table 5 depicts ACC and execution time (t_{exet}) need to complete all their tasks for a signal frame of no-noise signal and noise-adding signal of differential methods with the same data set.

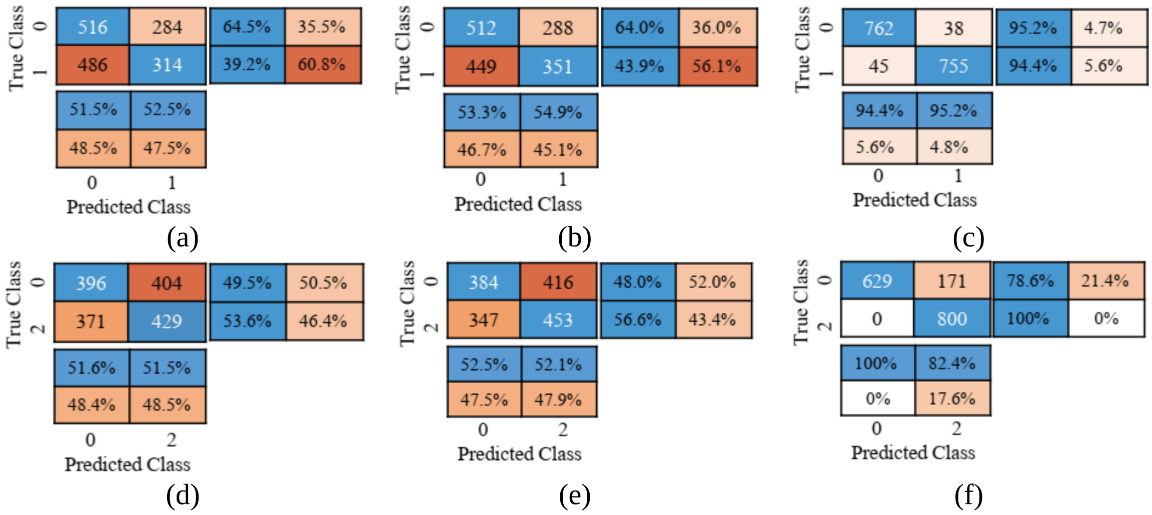

***Figure 6.** Confusion matrix of k-NN classifier by different methods: (a) K0-KA, DWT, (b) K0-KA, EMD, (c) K0-KA, the proposed method, (d) K0-KI, DWT, (e) K0-KI, EMD, (f) K0-KI, the proposed method with the noise-adding signal.*

***Table 5.** ACC and execution time of DWT method, EMD method and the proposed technique.*

Method	ACC between K0-KA	ACC between K0-KI	Average ACC	Execute time
	ACC with the no-noise signal			
DWT	60.12%	61.50%	60.81%	0.014 s
EMD	71.19%	70.38%	70.79%	0.040 s
Proposed	100%	100%	100%	0.004 s
	ACC with noise-adding signal			
DWT	51.88%	51.56%	51.72%	0.014 s
EMD	53.94%	52.31%	53.12%	0.040 s
Proposed	94.81%	89.31%	92.06%	0.004 s

4. CONCLUSIONS

This work presents a new technique to improve the bearing failure diagnosis of electric motors using the current signal. Traditional methods process signals in the signal-space whereas the proposed technique process signals in the feature-space using a Kalman filter to assess the real state of the bearings and eliminate noise. Experimental results show that the suggested technique is more optimal than existing techniques in both preciseness and accomplishment time, appropriate for run-time engine bearing failure detection applications. Due to the use of Kalman filter to estimate the state, the proposed method still achieves high accuracy even for noise-adding signals while the published methods have only high accuracy for no-noise signals. In addition, the proposed method does not directly interfere with the bearings as well as other components of the motor and the physical parameters of the bearings do not affect the accuracy of the calculation results. Consequently, the proposed technique could be applied for bearing condition classification of any electric machines in real-time.

REFERENCES

[1]. Singh GK. *"Induction machine drive condition monitoring and diagnostic research - a survey"*. Electr Power Syst Res; 64:145–58, (2003).

[2]. Bessous N, Sbaa S, Megherbi AC. *"Mechanical fault detection in rotating electrical machines using MCSA-FFT and MCSA-DWT techniques"*. Bull Pol Acad Sci Tech Sci 67 (2019).

[3]. Lei Y. *"Fault diagnosis of rotating machinery based on empirical mode decomposition. Struct. Health Monit"*. Adv. Signal Process. Perspect., Springer, p. 259–92, (2017).

[4]. Li Y, Xu M, Wang R, Huang W. *"A fault diagnosis scheme for rolling bearing based on local mean decomposition and improved multiscale fuzzy entropy"*. J Sound Vib 360:277–99 (2016).

[5]. Gu X, Chen C. *"Rolling bearing fault signal extraction based on stochastic resonance-based denoising and VMD"*. Int J Rotating; (2017).

[6]. Yan X, Jia M. *"A novel optimized SVM classification algorithm with multi-domain feature and its application to fault diagnosis of rolling bearing"*. Neurocomputing 313:47–64 (2018). https://doi.org/10.1016/j.neucom.2018.05.002.

[7]. He F, Ye Q. *"A Bearing Fault Diagnosis Method Based on Wavelet Packet Transform and Convolutional Neural Network Optimized by Simulated Annealing Algorithm"*. Sensors 22:1410 (2022). https://doi.org/10.3390/s22041410.

[8]. Chen FF, Li M, Chen BJ. *"Fault diagnosis of roller bearing based on hybrid feature set and weighted KNN"*. J Mech Transm 40:138–43 (2016).

[9]. Kang M, Kim J, Wills LM, Kim J-M. *"Time-Varying and Multiresolution Envelope Analysis and Discriminative Feature Analysis for Bearing Fault Diagnosis"*. IEEE Trans Ind Electron 62:7749–61 (2015). https://doi.org/10.1109/TIE.2015.2460242.

[10]. Kay SM. *"Fundamentals of statistical signal processing: estimation theory"*. Prentice-Hall, Inc.; (1993).

[11]. Brown RG, Hwang PY. *"Introduction to random signals and applied Kalman filtering: with MATLAB exercises and solutions"*. Introd Random Signals Appl Kalman Filter MATLAB Exerc Solut (1997).

[12]. Koutroumbas K, Theodoridis S. *"Pattern recognition"*. Academic Press; (2008).

[13]. Smith KJ. Precalculus: *"A functional approach to graphing and problem solving"*. Jones & Bartlett Publishers; (2011).

[14]. Lessmeier C, Kimotho JK, Zimmer D, Sextro W. *"Condition monitoring of bearing damage in electromechanical drive systems by using motor current signals of electric motors: A benchmark data set for data-driven classification"*. PHM Soc. Eur. Conf., vol. 3, (2016).

[15]. Hoang DT, Kang HJ. *"A Motor Current Signal-Based Bearing Fault Diagnosis Using Deep Learning and Information Fusion"*. IEEE Trans Instrum Meas 69:3325–33 (2020).

TÓM TẮT

Chẩn đoán lỗi vòng bi của máy điện sử dụng tín hiệu dòng điện động cơ và phân loại trạng thái

Quy trình chẩn đoán lỗi vòng bi của động cơ cảm ứng dựa trên tín hiệu dòng điện của động cơ trong các phương pháp đã công bố thường khử nhiễu tín hiệu thu được từ các cảm biến dòng điện, sau đó trích xuất các đặc tính điển hình từ tín hiệu đã khử nhiễu và sử dụng bộ phân loại để phân biệt trạng thái của vòng bi. Tuy nhiên, các tín hiệu dòng điện trong thực tế có thể bị ảnh hưởng bởi nhiễu tạp xung quanh, tạo ra các đỉnh bất thường trong tín hiệu có thể dẫn đến kết quả chẩn đoán không chính xác. Vì vậy, các phương pháp truyền thống có thể không hiệu quả lắm trong việc chẩn đoán lỗi động cơ cảm ứng sử dụng tín hiệu dòng điện động cơ trong thời gian thực. Để giảm thiểu những vấn đề này, công trình này giới thiệu một kỹ thuật mới, bao gồm mô hình hóa trạng thái của vòng bi dưới dạng một vectơ trạng thái chứa các đặc tính tín hiệu, đánh giá trạng thái thực của vòng bi trong không gian đặc tính bằng cách sử dụng bộ lọc Kalman và bộ phân loại k-NN. Kỹ thuật này vẫn đạt độ chính xác khá cao ngay cả trong điều kiện có nhiễu. Kết quả thử nghiệm với tín hiệu dòng điện có nhiễu chứng minh rằng kỹ thuật đề xuất có tỷ lệ nhận dạng đúng trung bình là 92,06% và tỷ lệ sai trung bình là 7,94%, trong khi các phương pháp thông thường có tỷ lệ nhận dạng đúng trung bình tối đa là 53,12% và tỷ lệ sai sót trung bình tối thiểu là 46,88%.

Từ khoá: Chẩn đoán lỗi vòng bi; Tín hiệu dòng điện động cơ; Phân loại trạng thái.